Interferometric control of absorption in thin plasmonic metamaterials: general two port theory and broadband operation

L. Baldacci,[1,2,*] **S. Zanotto,**[1,5] **G. Biasiol,**[3] **L. Sorba,**[1] **and A. Tredicucci**[4]

[1]*NEST, Istituto Nanoscienze - CNR and Scuola Normale Superiore, P.za S. Silvestro 12, 56127 Pisa, Italy*

[2]*Scuola Superiore Sant'Anna, Institute of Life Sciences, P.za Martiri della libertà 33, 56127 Pisa, Italy*

[3]*CNR-IOM, Laboratorio TASC, Area Science Park, I-34149 Trieste, Italy*

[4]*NEST, Istituto Nanoscienze - CNR and Dipartimento di Fisica "E. Fermi", Università di Pisa, Largo Pontecorvo 3, 56127 Pisa, Italy*

[5]*Present address: Dipartimento di Elettronica, Informazione e Bioingegneria, Politecnico di Milano, Via Colombo 81, 20133 Milano, Italy*

[*]*l.baldacci@sssup.it*

http://www.laboratorionest.it

Abstract: In order to extend the Coherent Perfect Absorption (CPA) phenomenology to broadband operation, the interferometric control of absorption is investigated in two-port systems without port permutation symmetry. Starting from the two-port theory of CPA treated within the Scattering Matrix formalism, we demonstrate that for all linear two-port systems with reciprocity the absorption is represented by an ellipse as function of the relative phase and intensity of the two input beams, and it is uniquely determined by the device single-beam reflectance and transmittance, and by the dephasing of the output beams. The basic properties of the phenomenon in systems without port permutation symmetry show that CPA conditions can still be found in such asymmetric devices, while the asymmetry can be beneficial for broadband operation. As experimental proof, we performed transmission measurements on a metal-semiconductor metamaterial, employing a Mach-Zehnder interferometer. The experimental results clearly evidence the elliptical feature of absorption and trace a route towards broadband operation.

OCIS codes: (260.3160) Interference; (160.3918) Metamaterials; (250.5403) Plasmonics.

References and links

1. Y. D. Chong, L. Ge, H. Cao, and A. D. Stone, "Coherent perfect absorbers: Time-reversed lasers," Phys. Rev. Lett. **105**, 053901 (2010).
2. S. Longhi, "Pt-symmetric laser absorber," Phys. Rev. A **82**, 031801 (2010).
3. Y. Sun, W. Tan, H.-q. Li, J. Li, and H. Chen, "Experimental demonstration of a coherent perfect absorber with pt phase transition," Phys. Rev. Lett. **112**, 143903 (2014).

#232139 - $15.00 USD Received 8 Jan 2015; revised 5 Mar 2015; accepted 23 Mar 2015; published 2 Apr 2015

4. S. M. Barnett, J. Jeffers, A. Gatti, and R. Loudon, "Quantum optics of lossy beam splitters," Phys. Rev. A **57**, 2134–2145 (1998).
5. J. Jeffers, "Interference and the lossless lossy beam splitter," Journal of Modern Optics **47**, 1819–1824 (2000).
6. S. Huang and G. Agarwal, "Coherent perfect absorption of single photons," arXiv preprint arXiv:1402.7146 (2014).
7. W. Wan, Y. Chong, L. Ge, H. Noh, A. D. Stone, and H. Cao, "Time-reversed lasing and interferometric control of absorption," Science **331**, 889–892 (2011).
8. S. Zanotto, F. P. Mezzapesa, F. Bianco, G. Biasiol, L. Baldacci, M. S. Vitiello, L. Sorba, R. Colombelli, and A. Tredicucci, "Perfect energy-feeding into strongly coupled systems and interferometric control of polariton absorption," Nature Phys. **10**, 830–834 (2014).
9. J. Yoon, K. H. Seol, S. H. Song, and R. Magnusson, "Critical coupling in dissipative surface-plasmon resonators with multiple ports," Opt. Express **18**, 25702–25711 (2010).
10. H. A. Haus, *Waves and fields in optoelectronics* (Prentice-Hall, 1984).
11. A. Yariv and P. Yeh, *Photonics: Optical Electronics in Modern Communication* (Oxford University, 2007).
12. M. Cai, O. Painter, and K. J. Vahala, "Observation of critical coupling in a fiber taper to a silica-microsphere whispering-gallery mode system," Phys. Rev. Lett. **85**, 74–77 (2000).
13. X. Liu, T. Tyler, T. Starr, A. F. Starr, N. M. Jokerst, and W. J. Padilla, "Taming the blackbody with infrared metamaterials as selective thermal emitters," Phys. Rev. Lett. **107**, 045901 (2011).
14. J.-M. Manceau, S. Zanotto, I. Sagnes, G. Beaudoin, and R. Colombelli, "Optical critical coupling into highly confining metal-insulator-metal resonators," Applied Physics Letters **103**, 091110 (2013).
15. Z. Yu, A. Raman, and S. Fan, "Thermodynamic upper bound on broadband light coupling with photonic structures," Phys. Rev. Lett. **109**, 173901 (2012).
16. M. Pu, Q. Feng, M. Wang, C. Hu, C. Huang, X. Ma, Z. Zhao, C. Wang, and X. Luo, "Ultrathin broadband nearly perfect absorber with symmetrical coherent illumination," Opt. Express **20**, 2246–2254 (2012).
17. R. Bruck and O. L. Muskens, "Plasmonic nanoantennas as integrated coherent perfect absorbers on soi waveguides for modulators and all-optical switches," Opt. Express **21**, 27652–27661 (2013).
18. J. A. Giese, J. W. Yoon, B. R. Wenner, J. W. Allen, M. S. Allen, and R. Magnusson, "Guided-mode resonant coherent light absorbers," Opt. Lett. **39**, 486–488 (2014).
19. J. W. Yoon, G. M. Koh, S. H. Song, and R. Magnusson, "Measurement and modeling of a complete optical absorption and scattering by coherent surface plasmon-polariton excitation using a silver thin-film grating," Phys. Rev. Lett. **109**, 257402 (2012).
20. J. R. Piper and S. Fan, "Total absorption in a graphene monolayer in the optical regime by critical coupling with a photonic crystal guided resonance," ACS Photonics **1**, 347–353 (2014).
21. G. Granet and B. Guizal, "Efficient implementation of the coupled-wave method for metallic lamellar gratings in tm polarization," J. Opt. Soc. Am. A **13**, 1019–1023 (1996).
22. W. C. Chew, *Waves and Fields in Inhomogeneous Media*, vol. 522 (IEEE, 1995).
23. D. Jalas, A. Petrov, M. Eich, W. Freude, S. Fan, Z. Yu, R. Baets, M. Popovic, A. Melloni, J. D. Joannopoulos, M. Vanwolleghem, C. R. Doerr, and H. Renner, "What is – and what is not – an optical isolator," Nature Photonics **7**, 579 – 582 (2013).
24. P. B. Johnson and R.-W. Christy, "Optical constants of the noble metals," Physical Review B **6**, 4370 (1972).
25. D. Aspnes and A. Studna, "Dielectric functions and optical parameters of si, ge, gap, gaas, gasb, inp, inas, and insb from 1.5 to 6.0 ev," Physical Review B **27**, 985 (1983).

1. Introduction

The issue of full optical switching, that is, controlling the flow of a light beam with another light beam, is a fundamental building block of optical networks. This kind of light modulation can be achieved in a multi-port lossy optical system, relying on the phenomenon named *coherent perfect absorption* (CPA). CPA consists of the complete dissipation of the input optical power occurring when the amplitude and phase of one input beam have a well-defined relation with the amplitudes and phases of the other beam(s), provided that the determinant of the scattering matrix of the system is vanishing. This phenomenon has a neat theoretical interpretation, as it corresponds to the time-reversal of a laser at threshold [1]. In addition, studies on the role of combined parity and time symmetries further highlight the potential of complex, multi-port optical devices [2,3], bringing CPA and related phenomena to the interest of a broad community in physics and engineering. While the above phenomena deal with classical wave optics, the extension of the CPA concept to the quantum world deserves an interest on its own, since an apparent two-photon absorption mechanism has been predicted to occur in properly tailored

#232139 - $15.00 USD Received 8 Jan 2015; revised 5 Mar 2015; accepted 23 Mar 2015; published 2 Apr 2015

linear absorbing beamsplitters [4–6].

The simplest CPA device is a symmetric, free-standing slab of absorbing material, whose thickness and (complex) refractive index are properly tuned to implement the zero determinant condition [7]; at the target resonance wavelength, light absorption into the slab can be modulated in full by means of the input beams dephasing. For off-resonance wavelengths the modulation is much smaller, and a CPA bandwidth can hence be defined. Indeed, this bandwidth is connected to the resonance decay time of the photonic resonator loaded by the non-radiative losses. In order to achieve the CPA condition these non-radiative losses need to be matched with the bare resonator radiative losses [8]. In other words, the CPA is the generalization to multi-port systems of the well known critical coupling condition [9], which plays a fundamental role in the optimization of a wide class of devices, from antennas and radiation detectors [10] to microresonators [11, 12], thermal emitters [13, 14], and solar cells [15].

To date, the majority of CPA devices that have been experimentally demonstrated exhibit a strict permutation symmetry between the two ports and a narrow bandwidth, and the proposals of wide-band CPA only have theoretical character [16, 17]. In the first part of this work, we report about a general analysis of coherent absorption modulation in two-port reciprocal systems, with a clear graphical interpretation of the role of device asymmetry, and point out some properties which can improve the device flexibility for broadband applications. Triggered by previous studies on periodic structures, either purely dielectric [18], purely metallic [19], or embedding graphene components [20], in the experimental part we propose to exploit the plasmonic resonance of a thin metal-dielectric metamaterial, consisting of a subwavelength titanium grating supported by a gallium arsenide membrane, to demonstrate coherent modulation of absorption over a bandwidth of $1/10$ of the central resonance frequency. Experimental evidence is provided, and supported by numerical simulations performed with rigorous coupled-wave analysis [21].

2. General theory of coherent control of absorption in two-port reciprocal systems

Consider a linear two-port system like that schematized in the upper left panel of Fig. 1, driven by coherent input beams through the ports, i.e., through the scattering channels. Outside the device, the electromagnetic field can be described by the complex amplitudes of input and output fields, $s^{\pm}_{1,2}$. Provided that a proper normalization is employed, these amplitudes are connected with the electromagnetic power flux entering or leaving the device: $I^{\text{in,out}}_{1,2} = |s^{\pm}_{1,2}|^2$. Depending on the physical system, the input and output ports correspond to plane waves (in the case of a multilayer), to diffraction channels (in the case of a grating), to waveguide modes (in the case of integrated optical circuits), or to more complex far-field wave patterns (like the spatial harmonics in systems which exhibit a cylindrical or spherical symmetry). The theory that follows handles in a general way all the above situations, provided that only two input/output channels are coupled at a time.

In terms of the scattering matrix, input and output amplitudes are related by

$$\begin{pmatrix} s^{-}_1 \\ s^{-}_2 \end{pmatrix} = S \begin{pmatrix} s^{+}_1 \\ s^{+}_2 \end{pmatrix} \tag{1}$$

where S depends on the device structure and on the frequency of the monochromatic input beams. Without loss of generality, if the system is reciprocal [22, 23] the scattering matrix can be parametrized as

$$S = e^{i\phi} \begin{pmatrix} \rho_1 e^{i\psi_1} & i\tau \\ i\tau & \rho_2 e^{i\psi_2} \end{pmatrix} \tag{2}$$

where $\rho^2_{1,2}$ are the reflectances and τ^2 is the transmittance of the device. Notice that for a system which is symmetric for the exchange of ports 1 and 2 one has $\rho_1 = \rho_2$ and $\psi_1 = \psi_2$.

#232139 - $15.00 USD Received 8 Jan 2015; revised 5 Mar 2015; accepted 23 Mar 2015; published 2 Apr 2015

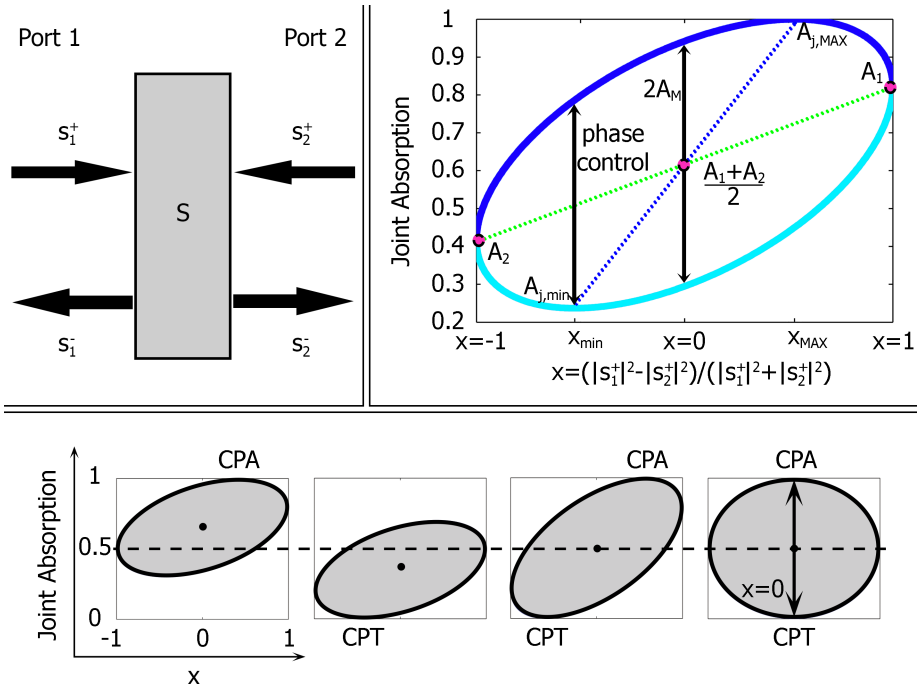

Fig. 1. Coherent absorption control in a linear two port scattering system with reciprocity. In the upper-left panel a general schematic is presented, with the scattering properties defined by a matrix S. If the two inputs are coherent, the total absorption $A_j = 1 - I_{out}/I_{in}$ can be controlled by means of their relative phase $\gamma = \arg(s_2^+/s_1^+)$ and access all values delimited by an ellipse as function of their normalized relative intensity $x = (|s_1^+|^2 - |s_2^+|^2)/(|s_1^+|^2 + |s_2^+|^2)$, as illustraded by the graph in the upper-right panel. For fixed x, absorption can assume all different values along the vertical line delimited by the ellipse simply varying the phase difference γ. On the contrary, total absorption in the presence of two incoherent inputs is described by a straightline connecting A_2 to A_1, with no possibility to be controlled by γ.

Being interested in the energy fluxes through the system, we write the total output intensity ($I^{\rm out} = I_1^{\rm out} + I_2^{\rm out}$) observed when the device is driven by two coherent fields dephased by $\gamma = \arg(s_2^+/s_1^+)$ as

$$I^{\rm out} = |s_1^-|^2 + |s_2^-|^2 = \\ (\rho_1^2+\tau^2)|s_1^+|^2 + (\rho_2^2+\tau^2)|s_2^+|^2 + 2|s_1^+||s_2^+|\tau\sqrt{\rho_1^2+\rho_2^2-2\rho_1\rho_2\cos(\psi_1+\psi_2)}\,\sin(\gamma+\delta). \tag{3}$$

The last term accounts for the interference induced by the coherent nature of the input beams. It depends on the input field dephasing, but also on a device-specific phase δ, which explicitly reads as

$$\tan\delta = \frac{\rho_2\sin(\psi_2)+\rho_1\sin(\psi_1)}{\rho_2\cos(\psi_2)-\rho_1\cos(\psi_1)}. \tag{4}$$

Defining the *joint absorption* as the fraction of energy absorbed when the system is driven by the coherent beams, from Eq. (3) and applying straightforward algebraic manipulation one

#232139 - $15.00 USD Received 8 Jan 2015; revised 5 Mar 2015; accepted 23 Mar 2015; published 2 Apr 2015

obtains

$$A_j = 1 - \frac{I^{\text{out}}}{I^{\text{in}}} = \\ \frac{1+x}{2}A_1 + \frac{1-x}{2}A_2 - \sqrt{1-x^2}\,A_M \sin(\gamma+\delta), \tag{5}$$

where

$$A_M = \sqrt{(1-A_1)(1-A_2) - |\det S|^2} \tag{6}$$

and

$$x = \frac{|s_1^+|^2 - |s_2^+|^2}{|s_1^+|^2 + |s_2^+|^2}. \tag{7}$$

Equation (5), which describes an ellipse in the plane (x, A_j) (see Fig. 1), encloses in a compact form a number of significant features. First, when the parameter x equals ± 1, i.e. when the system is driven from a single port, the joint absorbance reduces to the ordinary single-beam absorbances $A_{1,2} = 1 - \rho_{1,2}^2 - \tau^2$. As far as $|x|$ is moved toward smaller values, i.e., when the excitation becomes more symmetric, the absorbance is modulated by the input beams dephasing; the depth of such modulation is quantified by the parameter A_M. This phenomenon can be referred to as *coherent control of absorption*, and is a precursor of proper CPA. Analyzing Eq. (5), or Fig. 1, it turns out that the maximal absorption modulation always occurs when $x = 0$, regardless of the system asymmetry. Meanwhile, minimum and maximum joint absorption are reached when $x = x_{\text{min,max}}$, a symmetrically placed pair of points whose explicit expression is given by

$$\begin{aligned} x_{\text{min}} &= -x_{\text{max}} \\ x_{\text{max}} &= \pm\sqrt{\frac{(A_1-A_2)^2}{4A_M^2+(A_1-A_2)^2}} \end{aligned} \tag{8}$$

where the plus (minus) sign applies when $A_1 > A_2$ ($A_1 < A_2$).

In general, the minimum and maximum values of joint absorption are neither zero nor unity; consistently with the theory presented in [1], it can be shown that unity absorption occurs if and only if $\det S = 0$, also when the device is asymmetric (Fig. 1, lower panel). But instead of $\rho = \tau$, $\psi = (2m+1)\pi/2$ (m can be any integer number), the conditions on the scattering coefficients are now relaxed to $\tau^2 = \rho_1\rho_2$, $\psi_1 + \psi_2 = (2m+1)\pi$. Such device may also simultaneously show both unity and zero absorption (which we call *coherent perfect transparency*, CPT, in accordance to [8]); however, only a symmetric device allows for the sweep between CPA and CPT by a simple phase modulation. Recalling Eq. (4), it can be noticed that such a symmetric device exhibits CPA when the input beam dephasing is either $\gamma = 0$ or $\gamma = \pi$, as known from previous reports in the literature [1, 7].

By analyzing Fig. 1 (lower panels), a set of constraints on the single-beam absorbances can also be deduced. Indeed, in order to achieve the CPA, a passive device must show $(A_1+A_2)/2 > 0.5$; on the other hand, CPT is reachable only if $(A_1+A_2)/2 < 0.5$. The compresence of CPA and CPT requires the strict condition $(A_1+A_2)/2 = 0.5$, which is a significant relation in that it connects quantities accessible in an ordinary single-port excitation experiment with the device response to coherent excitation. The above relations are only necessary but not sufficient in order to observe CPA, since proper phase relations on the scattering matrix coefficients must also be fulfilled. They can be employed however in fast pre-screening single-beam experiments.

Another property related to the asymmetry of the system can be deduced from Eq. (6). We want to find the conditions upon which $A_M = 0$. Using Eq. (3), A_M can be rewritten as

$$A_M = \tau\sqrt{\rho_1^2 + \rho_2^2 - 2\rho_1\rho_2\cos(\psi_1 + \psi_2)}. \tag{9}$$

#232139 - $15.00 USD Received 8 Jan 2015; revised 5 Mar 2015; accepted 23 Mar 2015; published 2 Apr 2015

Apart from the solutions $\tau = 0$ and $\rho_1 = \rho_2 = 0$, introducing the variable

$$y = \frac{\rho_1^2 - \rho_2^2}{\rho_1^2 + \rho_2^2}, \tag{10}$$

a third solution is found to be

$$\cos(\psi_1 + \psi_2) = \frac{1}{\sqrt{1 - y^2}}, \tag{11}$$

which can be verified if and only if $y = 0$, that is to say, if $\rho_1 = \rho_2$. Indeed, the case of zero modulation can be avoided with asymmetric devices, which makes them more flexible for broadband applications.

3. Experimental evidence of a two-port broadband coherent absorber based on a plasmonic metamaterial

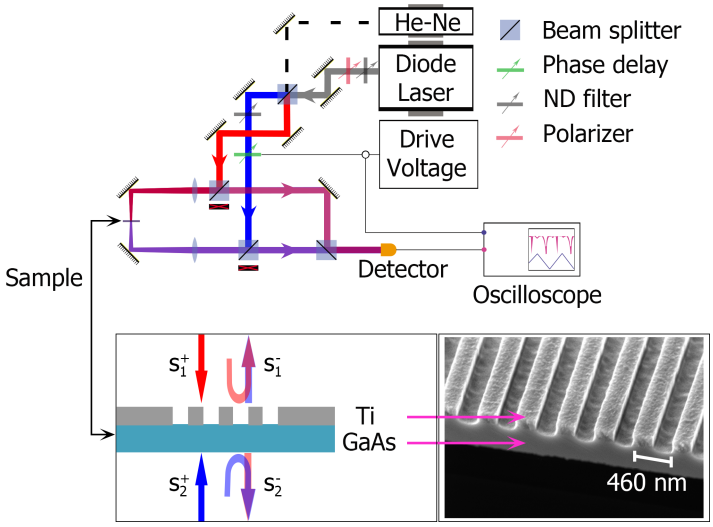

Fig. 2. Experimental setup and schematic of the sample. Radiation generated by a tunable diode laser is split in two and focused onto the opposite sides of the sample. The relative phase and intensity of the two input beams are controlled respectively by a neutral density filter wheel and a liquid crystal device driven by a voltage sweep. The total output intensity is then collected by a detector. A HeNe laser is employed for alignment purposes. Lower-right panel: SEM image of a cleaved sample.

As a prototype of broadband coherent absorber, we analyzed a thin plasmonic metamaterial based on the subwavelength grating geometry sketched in Fig. 2. It consists of a periodic array of titanium stripes lying on a gallium arsenide suspended membrane. The device is characterized by titanium and gallium arsenide thicknesses d_{Ti} and d_{GaAs}, by the periodicity a, and by the *filling fraction* f, which is defined as the ratio between the volume fraction of titanium an the volume fraction of air.

If the device is driven by two counterpropagating beams normally incident on the surface, it can be considered as a two-port device in the sense that only the zeroth diffraction order propagates in the far field outside the sample, according to the Helmholtz equation in vacuum. Inside,

#232139 - $15.00 USD Received 8 Jan 2015; revised 5 Mar 2015; accepted 23 Mar 2015; published 2 Apr 2015

a complex interplay between modes supported by the metal-air and metal-semiconductor interfaces leads to a broadband absorption band centered in the 900 - 1000 nm wavelength range. The fine tuning of the sample parameters d_{Ti}, d_{GaAs} and a relies on a numerical optimization of the CPA-related parameters A_M and $\det S$ introduced in the previous Section. As numerical modeling tool we employed the rigorous coupled-wave analysis (RCWA), in an implementation which ensures fast convergence for the TM polarization, i.e., when it is imposed that the sole $H \neq 0$ field component is that parallel to the pattern stripes [21]. From the simulations it turned out that the optimal parameters are $d_{\mathrm{Ti}} = 169$ nm, $d_{\mathrm{GaAs}} = 366$ nm, and $a = 457$ nm. The filling fraction f was not the object of optimization because $f = 0.5$ is the best value considering fabrication issues.

The sample is processed starting from a GaAs (001) wafer, on which a $\simeq 500$ nm thick $Al_{0.5}Ga_{0.5}As$ layer, followed by the 366 nm GaAs layer, are grown by molecular beam epitaxy. Then, the Ti layer is deposited via thermal evaporation, and the periodic pattern is defined on a $200 \times 200\ \mu m^2$ area by means of electron beam lithography and inductively-coupled plasma reactive ion etching. Finally, through a set of wet etching steps which exploit $Al_{0.5}Ga_{0.5}As$ as an etch-stop layer, the membrane is locally free from the substrate, and the plasmonic metamaterial can be optically accessed from both sides.

Experimental proof of broadband coherent absorption modulation is provided by measuring the total output intensity from the sample in presence of two counterpropagating input beams. To this aim, we built a Mach Zehnder interferometer, as shown in Fig. 2. As coherent light source, a Toptica DL100 grating-coupled diode laser, tunable from 908 to 983 nm, is employed; the beam is linearly polarized using a Glan Thompson $(200000:1)$ polarizer. After passing the first beamsplitter, the laser radiation is separated in two beams of approximately equal intensity. In order to explore the full dynamics predicted by the general theory of Section 2, we had to modulate the relative phase and intensity between the input beams. To this aim we placed a liquid crystal phase delay modulator across one of the two paths, and a filter wheel alternatively in one of the two paths. The two input beams are then focused using two achromatic doublets with 400 mm focal length, in a way that the two beam waists cover the sole patterned area of the sample. The output beams are eventually directed onto a detector; in order to avoid mutual interference of these beams on the detector surface, the two output paths are slightly displaced (not shown in the figure).

First proof of coherent control of absorption was observed for fixed laser wavelength $\lambda = 945$ nm. The results are shown in Fig. 3, where we plotted the two beam relative intensity on the horizontal axis, and the joint absorption on the vertical axis, in order to prove our theoretical predictions of Eq. (5).

The blue and light blue dots represent respectively the maximum and minimum experimental values of joint absorption. Following from Eq. (5), two ellipses are calculated. The dashed grey line is the ellipse resulting when the absorption coefficients are calculated through RCWA analysis, while the solid grey line is obtained by using the experimental values for A_1, A_2 and A_M. The general agreement between the experimental features of the joint absorption and the elliptical behavior predicted in the general theory clearly appears (Sect. 2 and Fig. 1). The disagreement between the RCWA calculations and the experimental results does not weaken the predictions of the general theory: the RCWA employed in this work derives the solution of Maxwell's equations for plane waves normally incident on a one dimensional grating made by perfectly vertical slabs, smooth surfaces, and materials having dielectric constants taken from the literature [24, 25]; more sophisticated methods which account for surface roughness and more complex spatial distribution of the incident radiation may improve the predictions on the fields and then on the scattering coefficients. Nevertheless, even if the sample does not show the full features expected by design, the elliptical behavior of joint absorption is preserved, as

#232139 - $15.00 USD Received 8 Jan 2015; revised 5 Mar 2015; accepted 23 Mar 2015; published 2 Apr 2015

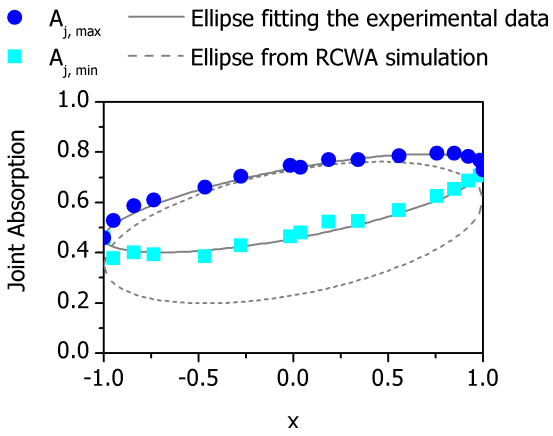

Fig. 3. Maximum and minimum joint absorption as function of input beams relative intensity. The elliptical feature predicted in the general theory (Sect. 2 and Fig. 1) is clearly observed in the experiment. The dashed line is obtained through the rigorous coupled wave analysis (RCWA). The mismatch with the measured set is attributed to the roughness of the interfaces resulting from the etching processes, the bending of the sample due to the strain at the interface between Ti and GaAs, the complex spatial distribution of the incident beams, which RCWA does not account for, in addition to the possible mismatch between the dielectric constants employed, taken from the literature [24, 25], and their actual values.

it is the signature of a general two port system, regardless of the particular values assumed for the scattering coefficients. The solid line ellipse has a fairly different meaning, as it is obtained from the experimental values of absorption. Once the single beam absorption and the modulation depth are known the experimental ellipse can be completely described.

In the second part of the experiment the broadband operation of the plasmonic metamaterial is demonstrated; the two input beam intensities are fixed to be equal, while the wavelength is swept across the accessible spectral range of the laser source. On the left side of Fig. 4, the experimental data are reported; again blue and light blue points represent the measured maximum/minimum absorption values, while the black points show the measured values for $(A_1 + A_2)/2$, i.e. the average of the single beam absorption values. This demonstrates that the symmetries reported in Fig. 3 are preserved for all the probed wavelengths. On the right side of Fig. 4, the RCWA calculations are presented, which predict coherent absorption control through the whole broad spectrum thanks to the plasmonic nature of the EM resonance. The reduced thickness of the sample combined with its heavy ohmic losses provided by the titanium stripes ensures in fact a broad resonance, with A_1 and A_2 sufficiently high, while the phase difference between the two output beams varies smoothly by moving the wavelength away from resonance [9]. A similar behavior was observed experimentally for all the eleven selected wavelengths. The disagreement between experimental data and theoretical calculations could be traced back to possible back-reflections of the input laser beams into the diode cavity; the corresponding instabilities of emitted power likely lead to a partial deformation of the scattering spectrum. For this reason, a precise range of the achieved modulation bandwidth cannot be stated, although it roughly spans tens of nanometers. It is important to note that the measured single beam absorbances are consistent with the measured $A_{j,max}$ and $A_{j,min}$ within a two port picture of the system. Even if the modulation depth is not as pronounced as the RCWA predictions, it is observed through the whole spectrum considered. The absorption is maximally modulated at $\lambda = 945$ nm, with an excursion of 30%, while the extremes of the spectrum, $\lambda = 908$ nm and

#232139 - $15.00 USD Received 8 Jan 2015; revised 5 Mar 2015; accepted 23 Mar 2015; published 2 Apr 2015

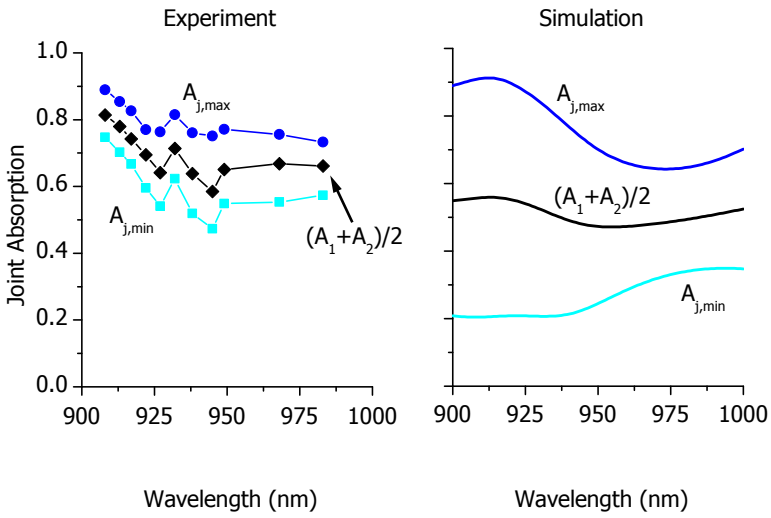

Fig. 4. Joint absorption spectrum, experimental results (left) and theoretical predictions (right) obtained through RCWA. Incident beams have fixed equal intensity. In both cases the symmetry predicted in the general two port theory is preserved. The broad operation band is attributed to the plasmonic resonance of the sample. The disagreement between measured and predicted values is due to the back-reflection of signal into the cavity of the laser as the sample is put into the setup.

$\lambda = 983$ nm, still exhibit an excursion of 15% and 20% respectively.

4. Conclusion

In summary, we developed an analysis on two-port reciprocal systems without permutation symmetry between the two ports, which usually applies to this class of devices. We found that, regardless of geometry, absorption features and far-field wavepattern, the joint absorption is represented by an ellipse as function of three experimentally accessible parameters: the absorptions related to single port input, and the modulation depth when the two input beams have equal intensity. Moreover, CPA conditions are loosen and the condition of zero absorption modulation can be avoided. Using a metal-dielectric metamaterial we have observed the predicted elliptical feature of absorption, confirming it as an easy-to-use test for full characterization of samples whose working principle is the coherent control of absorption. Relying on plasmonic resonances in the near infrared spectral region, broadband coherent absorption control has been observed with an operational bandwidth of $\sim 1/10$ the central wavelength. Although the experimental results on broadband control of absorption suffered strong deviations from the RCWA calculations, they prove that asymmetric devices can be a flexible alternative to symmetric devices.

Acknowledgments

This work was supported by the European Research Council through the advanced grant No. 321122 SouLMan. We thank Alessandro Pitanti for helpful discussions.

#232139 - $15.00 USD Received 8 Jan 2015; revised 5 Mar 2015; accepted 23 Mar 2015; published 2 Apr 2015